COMMUNICATIONS

Magnetic Resonance in Medicine 44:169–173 (2000)

Imaging Blood Flow in Brain Tumors Using Arterial Spin Labeling

Afonso C. Silva,* Seong-Gi Kim, and Michael Garwood

Measurements of tumor blood flow (TBF) are important for understanding tumor physiology and can be valuable in selecting and evaluating therapies. Brain tumors typically present reduced blood flows compared to normal brain tissue. This study shows that the arterial spin labeling (ASL) technique can be used to measure TBF non-invasively in a rat glioma model. Results show that TBF in the core (36.3 ± 18.9 ml/100g/min, n=4) and peripheral regions (85.3 ± 26.9 ml/100g/min, n=4) of the tumor are significantly reduced and show considerable heterogeneity compared to cerebral blood flow (CBF) of normal brain tissue (147.7 ± 31.1 ml/100g/min, n=4), while T_1 in the tumor (2.6 ± 0.1sec) is significantly elevated compared to normal tissue T_1 (2.0 ± 0.0 sec). These results strongly support the feasibility of using the ASL technique to evaluate different cancer treatment strategies, to monitor the effects of agents designed to modulate TBF and oxygenation (e.g., carbogen gas), and to assess and guide the use of anti-angiogenic agents. Magn Reson Med 44:169–173, 2000. © 2000 Wiley-Liss, Inc.

Key words: angiogenesis; cerebral blood flow; glioma rat brain; tumor necrosis

Measurements of tumor blood flow (TBF) are important for understanding tumor physiology and can be valuable in selecting and evaluating therapies. For example, the selective sensitization of tumors to hyperthermia is generally ascribed to the poor tumor blood flow relative to surrounding normal tissue (1). Radiation therapy preferentially kills those cells that contain substantial amounts of dissolved oxygen (i.e., high blood flow), while anoxic or hypoxic tumor cells are relatively radiation-resistant. Furthermore, stimulation of angiogenesis can rapidly increase blood vessel density in tumors by as much as 10-fold (2). Therefore, quantitative measurements of TBF are needed to evaluate the effectiveness of new anti-angiogenic therapies and to tailor such therapies to individual tumors (3–6).

To determine TBF, deuterium NMR methods in conjunction with injection of deuterated water as a freely diffusible tracer have been employed (7–10). Although these methods can provide absolute TBF in whole tumor, the sensitivity of deuterium is not high enough to allow imaging of TBF with high spatial resolution, an essential step towards understanding the spatial distribution of blood flow in the tumor. In addition, the injection of exogenous tracer hinders repeated measurements in the same tumor. To overcome these problems, arterial spin-labeling (ASL) techniques can be employed using arterial blood water as a perfusion tracer. These techniques have been used extensively to image and quantitate cerebral blood flow (CBF) with the spatial resolution of a conventional ^{1}H MR image (11). These methods have the advantage of being completely non-invasive, of not requiring the use of contrast agents or other exogenous tracers, and of allowing the measurement to be repeated as often as desired, therefore providing dynamic information with high temporal resolution. The ASL methods perform well when the blood flow is sufficiently high so that the tagged spins reach the tissue within a transit time comparable to T_1. Since tumor blood flow is usually low (i.e., long transit time), it is interesting to verify whether ASL techniques can be applied to image and quantify blood flow in tumors. In a recent study, Brown et al. used ASL to measure tumor blood flow modulations induced by nicotinamide at 4.7 T (12). In their study, however, the quality of the TBF maps obtained was not sufficient to allow a clear distinction of areas containing diseased tissue from normal brain regions.

The purpose of the present study is to show that continuous ASL performed with a two-coil system in a high magnetic field (9.4 T) provides sufficient sensitivity to measure TBF in a rat glioma model. A high-resolution spin-echo technique with a 200 × 200 μm^2 in-plane resolution was used to obtain the TBF maps. We observed considerable heterogeneity of TBF within the tumor region, and high blood flows in the periphery of tumors. Our results show that the ASL technique can be utilized to map tumor blood flow quantitatively and repeatedly with high spatial resolution.

MATERIALS AND METHODS

Inoculation of Glioma Cells

For tumor implantation, 9L gliosarcoma cells were grown in culture using Eagle's minimal essential media (MEME) supplemented with 10% fetal bovine serum and Penicillin-Streptomycin antibodies. Cultures were maintained in a humidified atmosphere under 5% CO_2. Cells were harvested during log phase growth by brief exposure to 0.25% trypsin-EDTA and were washed and reconstituted in MEME to a concentration of 1×10^5 cells/μl. Male Fisher rats (F344, body weight ~200 g) were anesthetized with 0.25 ml/100 g I.M. of a 1:1:4 mixture of acepromazine (10 mg/ml), xylazine (20 mg/ml), and ketamine (100 mg/ml). Animals were placed in a stereotaxic device and a

Center for Magnetic Resonance Research, Department of Radiology, University of Minnesota Medical School, Minneapolis, Minnesota.

Grant sponsors: W.M. Keck Foundation; NIH; Grant numbers: CA64338; RR08079.

*Correspondence to: Afonso C. Silva, Ph.D., Laboratory of Functional and Molecular Imaging, National Institute of Neurological Disorders and Stroke, National Institutes of Health, 9000 Rockville Pike, Building 10, Room B1D69, Bethesda, MD 20892-1060. E-mail: silvaa@ninds.nih.gov

Received 6 December 1999; revised 17 March 2000; accepted 19 April 2000.

small hole was drilled on the right side of the skull, 4–5 mm from the midline and 2 mm posterior to the bregma. A 10 μl cell suspension was injected to a depth of 2–3 mm. The calvarial defect was sealed with bone wax.

MRI Methods

MRI measurements were performed in four animals, 12 to 17 days after the intracerebral inoculation of 9L gliosarcoma cells. The four rats used in this study were sedated with a 50% O_2 : 50% N_2O gas mixture containing 5% halothane. The animals were then orally intubated, and anesthesia was reduced and maintained at 1% throughout the duration of the experiments. The earpieces and bite-bar of a home-built stereotaxic head holder secured the head of the animals, which were then placed in the magnet. Rectal temperature was maintained at 37 ± 0.1°C by means of a feedback controlled heated water pad.

Experiments were performed on a 9.4 T/31 cm horizontal magnet (Magnex, UK) interfaced to a UNITY INOVA console (Varian, CA). A double spin-echo sequence using adiabatic pulses (13) was utilized in all imaging measurements. This sequence uses a non-selective adiabatic 90° RF pulse for excitation, followed by two slice-selective adiabatic 180° RF pulses for refocusing of the echo (13). Imaging parameters were: TR/TE = 3035/27 ms, NEX=1, FOV = 2.56 × 1.28 cm^2, slice thickness of 2 mm, and matrix size = 128 × 64 (nominal resolution of 200 × 200 × 2000 μm^3). The total acquisition time per image was approximately 3.25 min. The typical signal-to-noise ratio of each image was 150:1.

Continuous ASL was performed using a two-coil approach (14). A 0.5 cm diameter butterfly RF coil was used underneath the neck of the animal to label the arterial spins. This labeling coil was positioned 2 cm away from the imaging coil, which consisted of a 1.6 cm diameter surface coil (15,16). For the ASL images, a 3 sec labeling RF pulse was applied to the neck coil, in the presence of a 10 mT/m longitudinal gradient, prior to the acquisition of each *k*-space line of the double spin-echo sequence. For the control images, the sign of the offset-frequency used for labeling was switched. Each ASL experiment consisted of a pair of one labeled image and one control image. For each animal, two pairs were acquired before, and two acquired after the T_1 map was obtained. The four perfusion maps were then averaged for signal-to-noise, and to account for any variations in CBF or TBF during the acquisition of the T_1 map.

T_1 maps were obtained using the same double spin-echo sequence, with the same spatial resolution and TE as for the perfusion images. The repetition time was increased to TR = 11 sec and the inversion times used were TI = 0.1, 0.5, 2, 5 and 10 sec. A three-parameter fit was used to obtain the T_1 maps.

Once the T_1 maps and the control and labeled images were obtained, tissue blood flow images were formed according to (17):

$$TBF = \frac{\lambda}{T_1} \cdot \frac{S_{control} - S_{label}}{2\alpha \cdot S_{control}} \quad [1]$$

where λ = 0.9 is the tissue:blood partition coefficient for water; $S_{control}$ is the control image signal intensity; S_{label} is the labeled image signal intensity; T_1 is the T_1 map and α = 0.8 is the degree of labeling efficiency (14). Eq. [1] neglects the effects of cross-relaxation between water and tissue macromolecules (17). However, this has been shown to be a small effect. The calculation of CBF requires a knowledge of the regional tissue:blood partition coefficient. We assumed a constant value for the tissue:blood partition coefficient for water, λ (18). The implications of this assumption to our TBF measurements are evaluated in the Discussion section.

RESULTS

Figure 1 shows anatomical double spin-echo images (Fig. 1a), the corresponding T_1 maps (Fig. 1b), and calculated TBF maps (Fig. 1c) for the four animals used in this study. The slices were acquired through the center section of the tumor. Signal intensity within the tumors was relatively uniform in the spin-echo images (Fig. 1a). The needle track created by cell inoculation is visible in rats 1–3 and appears hypo-intense in these T_2 weighted images due to extravasation of deoxygenated red blood cells. With the exception of rat 4, the tumors developed just below the needle track and occupied primarily the striatum. Most of the tumor in rat 4 developed in the cerebral cortex around the injection site. While the tumors usually were confined to the ipsi-lateral cortex, rat 1 presented a tumor that advanced well into the contra-lateral cortex. T_1 was significantly elevated, albeit uniform, in the tumor regions, as compared with normal tissue (Fig. 1b). From the T_1 maps it is possible to delineate the apparent boundaries of the tumors. The T_1 maps also show the lateral ventricles as regions of bright intensity (Fig. 1b). The TBF maps (Fig. 1c) exhibited substantial heterogeneity (variation) in the tumors (see Table 1). The lowest blood flows were generally observed in the tumor core. The outer regions of the tumors typically exhibited higher TBF than the core, but lower flows than surrounding brain. From Fig. 1c it can be seen that the regions of altered blood flow extend beyond the regions of elevated T_1 values. For example, rats 3 and 4 show regions of decreased TBF below the tumor core, where T_1 values are apparently normal.

Table 1 compares T_1 and TBF in the tumor core, periphery, and normal brain tissue. T_1 was significantly increased in the tumor as compared to normal tissue ($P < 0.002$), whereas TBF was significantly reduced with respect to the CBF in normal brain tissue ($P < 0.02$). The tumor core presented the largest T_1 values. On the other hand, TBF was significantly reduced in the core. This inverse relationship between TBF and T_1 can be better observed in Fig. 2, where progressively longer T_1 values and correspondingly lower CBF (or TBF) values are found in normal tissue, tumor periphery and tumor core, respectively (Fig. 2). The correlation coefficient between TBF and T_1 values was −0.95.

DISCUSSION

The data presented here demonstrate an ability to image tumor perfusion with the ASL technique at a high magnetic field (9.4 T). TBF in the tumors is reduced, but measurable, compared to normal brain tissue. Further-

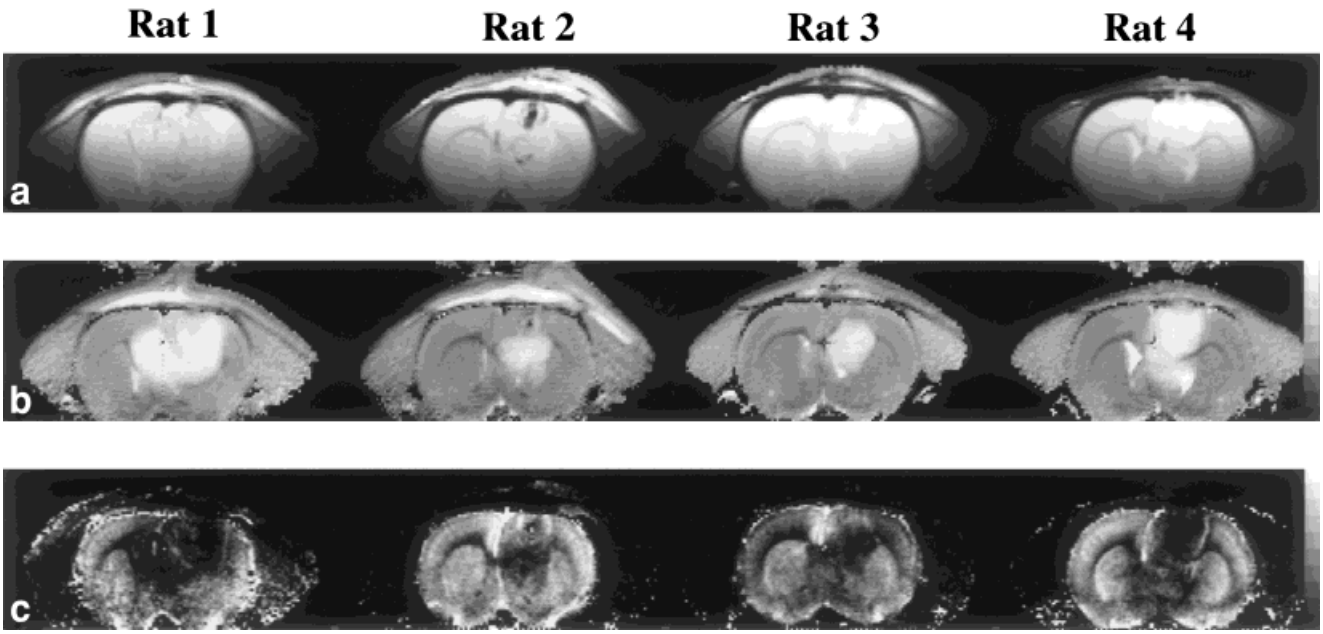

FIG. 1. **a:** Anatomical spin-echo coronal images containing the tumors, obtained from the four rats used in this study. The slices were acquired through the center section of the tumor. **b:** Corresponding T_1 maps obtained from the respective images shown in **a**. T_1 was significantly elevated, albeit uniform, in the tumor regions, as compared with normal tissue (grayscale bar: 1–3 sec). **c:** Corresponding perfusion images. Tumor blood flows were significantly reduced with respect to CBF in the normal brain tissue. The TBF maps exhibited substantial heterogeneity in the tumors. The lowest flows were generally observed in the tumor core. The periphery of the tumors showed higher TBF than the core, but lower blood flows than normal tissue (grayscale bar: 0–300 ml · 100 g^{-1} · min^{-1}).

more, we observed considerable heterogeneity in TBF values inside the tumors, consistent with previous work (19). The ASL technique used in this study provided sufficient sensitivity to visualize TBF in different pathologic tissue regions.

The proper quantification of CBF with the ASL technique depends on a series of parameters, as described by Eq. [1]. In particular, it depends on obtaining an accurate measurement of the labeling efficiency α, of the tissue T_1, and of the partition coefficient λ. While the measurements of α and T_1 are straightforward, measuring the partition coefficient λ is more elaborate, and involves dividing the proton density map of the tissue by the proton density map of blood water (20). In this work, we did not perform such measurement, and used a constant value for λ. This may lead to errors in the TBF measurements, because the partition coefficient changes significantly in brain tumors (21–23). In particular, our TBF measurements would be overestimated, or underestimated, if the actual value for the partition coefficient in the tumor is significantly smaller, or larger, respectively, in the tumor region, compared to the assumed value of 0.9. In fact, there are reports

Table 1
Comparison of T_1 and TBF in the Core and Peripheral Tumor Regions to T_1 and CBF in the Normal Contra-Lateral Brain*

	Tumor core		Tumor periphery		Normal contra-lateral white matter	
	T_1[a] (s)	TBF[b] (ml/100 g/min)	T_1[c] (s)	TBF[d] (ml/100 g/min)	T_1 (s)	CBF (ml/100 g/min)
Rat # 1	2.7 ± 0.1	26.0 ± 24.0	2.4 ± 0.3	48.0 ± 38.0	2.1 ± 0.1	105.8 ± 33.2
Rat # 2	2.5 ± 0.1	55.0 ± 23.0	2.2 ± 0.2	111.0 ± 54.0	1.9 ± 0.1	180.7 ± 25.6
Rat # 3	2.5 ± 0.1	49.0 ± 23.0	2.2 ± 0.3	86.0 ± 65.0	2.0 ± 0.1	154.2 ± 27.1
Rat # 4	2.7 ± 0.1	15.0 ± 18.0	2.3 ± 0.2	96.0 ± 63.0	1.9 ± 0.1	150.2 ± 34.4
Mean ± SD[e]	2.6 ± 0.1	36.3 ± 18.9	2.3 ± 0.1	85.3 ± 26.9	2.0 ± 0.1	147.7 ± 31.1

*Numbers represent mean ± SD inside ROIs drawn in corresponding regions of the tumor and contra-lateral normal brain tissue. ROI variability (SD/mean × 100) was 75% for tumor core; 67% for tumor periphery and 22% for normal brain white-matter tissue.
[a]T_1 values in the tumor core are significantly higher than T_1 in the tumor periphery and in normal brain tissue ($P < 0.002$).
[b]TBF values in tumor core are significantly lower than TBF in the tumor periphery and than CBF in normal brain white-matter tissue ($P < 0.02$).
[c]T_1 values in the tumor periphery are significantly higher than T_1 in normal brain tissue ($P < 0.005$).
[d]TBF values in tumor periphery are significantly lower than CBF in normal brain white-matter tissue ($P < 0.04$).
[e]Numbers in this row represent mean ± SD across the 4 animals.

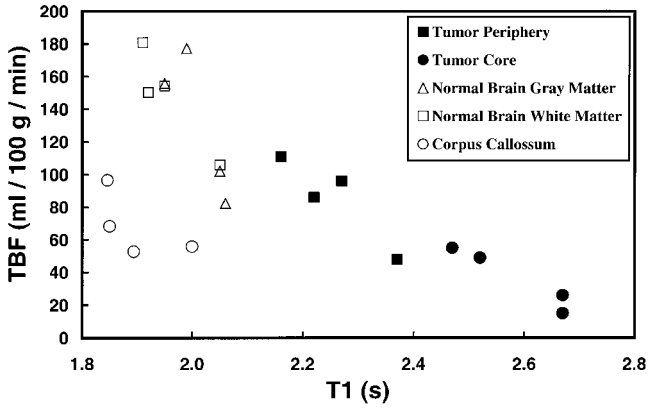

FIG. 2. Plot of TBF versus T_1. There is an inverse relationship between TBF and T_1. Tumor regions (closed circles and squares) presented longer T_1 values and lower blood flows than normal tissue (open symbols). The correlation coefficient between TBF and T_1 values was −0.95.

of elevated partition coefficient in tumors. For example, subcutaneous murine R1F-1 tumors have a tumor-to-blood partition coefficient of 0.94 (9), while rat C_6 gliomas show a partition coefficient of 0.994 (24). However, the main goal of this preliminary study was to investigate whether it would be possible to measure TBF using the ASL technique, which we have clearly achieved. Since the tumor-to-blood partition coefficient for water is expected to be in the range of 0.9–1, the maximum error induced by its variation should not exceed 10 %.

Two other sources of errors in the quantitation of CBF include the extraction fraction for water across the blood-tumor barrier, and the transit time of blood to move from the labeling plane to the exchange site. Although it is possible to measure extraction fractions with the ASL method (25,26), and thus calculate the permeability-surface area product of the tumor, it is unlikely that tumors have decreased extraction fractions, due to the lower TBF in the core, and to the leaky blood-tumor barrier (27). However, the transit-time can be significantly elongated due to the lower TBF. Nevertheless, transit-times in rats are small (~200 ms) (28) compared to T_1 of arterial water (~2.3 sec at 9.4 T), and thus small variations in transit-times should not introduce significant errors to the quantitation of TBF.

The T_1 inside the tumor regions was significantly higher than in normal brain tissue, while TBF was significantly lower than normal brain CBF. This inverse relationship between T_1 and TBF, shown in Fig. 2, runs over a much wider range in T_1 values than the T_1 variation of normal tissue, and cannot be attributed solely to the inverse CBF $\times$ T_1 relationship described by Eq. [1]. In fact, if one were to use Eq. [1] to extrapolate the CBF in normal brain tissue to the long T_1 values of tumors, one would find negative CBF values, i.e., the slope of the CBF $\times$ T_1 curve predicted by Eq. [1] is much steeper than the relation shown in Fig. 2. The increased T_1 values within the tumor regions are also related to changes in water content and molecular dynamics at the cellular level. On the other hand, the different TBF values inside the tumor are potentially more suggestive of the viability of the region, with the core being the most compromised region. This means the long T_1 values found in tumors are dissociated from their low TBF values, and therefore both T_1 maps as well as TBF maps are two independent, yet complementary ways to identify and classify brain tumor regions.

In summary, at high field ASL affords sufficient sensitivity to resolve perfusion heterogeneities in rat brain tumors. Besides its potential value for investigating the relationships between perfusion, physiology, and metabolism in tumors, the ability to measure TBF raises the possibility of using this technique to evaluate different treatment strategies. The ASL technique is expected to be useful for monitoring the effects of agents designed to modulate TBF and oxygenation (e.g., carbogen gas) and for evaluating and guiding the use of anti-angiogenic agents.

ACKNOWLEDGMENTS

The authors thank Dr. Joseph Lin for implanting the tumors and for assistance with animal preparation.

REFERENCES

1. Hetzel FW. Biologic rationale for hyperthermia. Radiol Clin North Am 1989;27:499–508.
2. Dellian M, Witwer BP, Salehi HA, Yuan F, Jain RK. Quantitation and physiological characterization of angiogenic vessels in mice: effect of basic fibroblast growth factor, vascular endothelial growth factor/vascular permeability factor, and host microenvironment. Am J Pathol 1996;149:59–71.
3. Behrens PF, Ostertag CB, Warnke PC. Regional cerebral blood flow in peritumoral brain edema during dexamethasone treatment: a xenon-enhanced computed tomographic study. Neurosurgery 1998;43:235–240.
4. Bondestam S, Halavaara JT, Jaaskelainen JE, Kinnunen JJ, Hamberg LM. Perfusion CT of the brain in the assessment of flow alterations during brachytherapy of meningioma. Acta Radiol 1999;40:469–473.
5. Johansson M, Bergenheim AT, Henriksson R, Koskinen LO, Vallbo C, Widmark A. Tumor blood flow and the cytotoxic effects of estramustine and its constituents in a rat glioma model. Neurosurgery 1997;41:237–243.
6. Nomura T, Ikezaki K, Natori Y, Fukui M. Altered response to histamine in brain tumor vessels: the selective increase of regional cerebral blood flow in transplanted rat brain tumor. J Neurosurg 1993;79:722–728.
7. Eskey CJ, Koretsky AP, Domach MM, Jain RK. 2H-nuclear magnetic resonance imaging of tumor blood flow: spatial and temporal heterogeneity in a tissue-isolated mammary adenocarcinoma. Cancer Res 1992; 52:6010–6019.
8. Kim S-G, Ackerman JJH. Multicompartment analysis of blood flow and tissue perfusion employing D2O as a freely diffusible tracer: a novel deuterium NMR technique demonstrated via application with murine RIF-1 tumors. Magn Reson Med 1988;8:410–426.
9. Kim S-G, Ackerman JJH. Quantitative determination of tumor blood flow and perfusion via deuterium nuclear magnetic resonance spectroscopy in mice. Cancer Res 1988;48:3449–3453.
10. Larcombe McDouall JB, Evelhoch JL. Deuterium nuclear magnetic resonance imaging of tracer distribution in D2O clearance measurements of tumor blood flow in mice. Cancer Res 1990;50:363–369.
11. Calamante F, Thomas DL, Pell GS, Wiersma J, Turner R. Measuring cerebral blood flow using magnetic resonance imaging techniques. J Cereb Blood Flow Metab 1999;19:701–735.
12. Brown SL, Ewing JR, Kolozsvary A, Butt S, Cao Y, Kim JH. Magnetic resonance imaging of perfusion in rat cerebral 9L tumor after nicotinamide administration. Int J Radiat Oncol Biol Phys 1999;43:627–633.
13. Schupp DG, Merkle H, Ellermann JM, Ke Y, Garwood M. Localized detection of glioma glycolysis using edited 1H MRS. Magn Reson Med 1993;30:18–27.

14. Silva AC, Zhang W, Williams DS, Koretsky AP. Multi-slice MRI of rat brain perfusion during amphetamine stimulation using arterial spin labeling. Magn Reson Med 1995;33:209–214.
15. Silva AC, Lee SP, Yang G, Iadecola C, Kim SG. Simultaneous blood oxygenation level-dependent and cerebral blood flow functional magnetic resonance imaging during forepaw stimulation in the rat. J Cereb Blood Flow Metab 1999;19:871–879.
16. Silva AC, Kim S-G. A pseudo-continuous arterial spin labeling technique for measuring CBF dynamics with high temporal resolution. Magn Reson Med 1999;42:425–429.
17. Zhang W, Silva AC, Williams DS, Koretsky AP. NMR measurement of perfusion using arterial spin labeling without saturation of macromolecular spins. Magn Reson Med 1995;33:370–376.
18. Herscovitch P, Raichle ME. What is the correct value for the brain—blood partition coefficient for water? J Cereb Blood Flow Metab 1985; 5:65–69.
19. Kuroda K, Skyhoj OT, Lassen NA. Regional cerebral blood flow in various types of brain tumor. Effect of the space-occupying lesion on blood flow in brain tissue close to and remote from tumor site. Acta Neurol Scand 1982;66:160–171.
20. Roberts DA, Rizi R, Lenkinski RE, Leigh JSJ. Magnetic resonance imaging of the brain: blood partition coefficient for water: application to spin-tagging measurement of perfusion. J Magn Reson Imaging 1996;6: 363–366.
21. Hiraga S, Klubes P, Owens ES, Cysyk RL, Blasberg RG. Increases in brain tumor and cerebral blood flow by blood-perfluorochemical emulsion (Fluosol-DA) exchange. Cancer Res 1987;47:3296–3302.
22. Nasel C, Rossler K, Heimberger K, Gorzer H, Lassmann H, Schindler E. Tumour blood flow and partition coefficients: correlation with grade of cerebral gliomas using xenon-enhanced computed tomography. Neuroradiology 1997;39:627–632.
23. Tachibana H, Meyer JS, Rose JE, Kandula P. Local cerebral blood flow and partition coefficients measured in cerebral astrocytomas of different grades of malignancy. Surg Neurol 1984;21:125–131.
24. Ross BD, Mitchell SL, Merkle H, Garwood M. In vivo 31P and 2H NMR studies of rat brain tumor pH and blood flow during acute hyperglycemia: differential effects between subcutaneous and intracerebral locations. Magn Reson Med 1989;12:219–234.
25. Silva AC, Williams DS, Koretsky AP. Evidence for the exchange of arterial spin-labeled water with tissue water in rat brain from diffusion-sensitized measurements of perfusion. Magn Reson Med 1997;38:232–237.
26. Silva AC, Zhang W, Williams DS, Koretsky AP. Estimation of water extraction fractions in rat brain using magnetic resonance measurement of perfusion with arterial spin labeling. Magn Reson Med 1997;37:58–68.
27. Kenney J, Schmiedl U, Maravilla K, Starr F, Graham M, Spence A, Nelson J. Measurement of blood-brain barrier permeability in a tumor model using magnetic resonance imaging with gadolinium-DTPA. Magn Reson Med 1992;27:68–75.
28. Zhang W, Williams DS, Detre JA, Koretsky AP. Measurement of brain perfusion by volume-localized NMR spectroscopy using inversion of arterial water spins: accounting for transit time and cross-relaxation. Magn Reson Med 1992;25:362–371.